ChemComm

COMMUNICATION

View Article Online
View Journal | View Issue

Cite this: *Chem. Commun.*, 2021, **57**, 12175

Received 26th August 2021,
Accepted 26th October 2021

DOI: 10.1039/d1cc04765e

rsc.li/chemcomm

Redox-induced reversible P–P coupling in a uranium complex†

Wei Fang,[a] Ambre Carpentier,[b] Xiong Sun,[a] Yue Zhao,[a] Laurent Maron*[b] and Congqing Zhu*[a]

A synthesized redox-active multidentate N–P ligand reacted with UCl_4 in the presence of KHMDS or ^{n}BuLi, where two novel U(IV) complexes with or without P–P coupling were formed, respectively. The reversible P–P coupling in these complexes was observed in redox-induced reactions.

Redox-active ligands play important roles in organometallic chemistry and exhibit reaction pathways different from traditional "innocent" ligands. Redox-active ligands are common in the chemistry of transition metals,[1] but their applications in actinide organometallic chemistry are rare. In recent years, only a few redox-active ligands, such as pyridine(diimine), bipyridines, α-diimine and mesitylene, have been investigated in uranium chemistry.[2] Bart and co-workers studied the redox chemistry of uranium and uranyl complexes with different kinds of redox-active ligands.[2d,3] Arnold and co-workers reported relatively rare inner- and outer-sphere reduction reactions supported by a redox-active dipyrrin in uranyl complexes.[4]

The coupling of the ligands in uranium chemistry is also an interesting but less frequently observed process. For example, Diaconescu and co-workers reported the C–C coupling of two coordinated 1-methylimidazole or 1-methylbenzimidazole in uranium systems.[5] A reversible C–C coupling in a uranium complex with Schiff base ligands was reported by Mazzanti and co-workers,[6] in which the C–C bond formation or cleavage could be promoted by the reduction or oxidation of the Schiff base ligands. Meyer and co-workers also found the C–C coupling in terminal alkynes through a uranium(III)-mediated process.[7] In addition, Zi and co-workers discovered the C–C coupling of two molecules of PhCH=NPh during their study of the reactivity of a uranium metallacyclopropene.[8] Recently, the Hayton group reported N–N and C–C coupling between the redox-active calix[4]pyrrole ligand in uranyl systems.[9] However, the redox-induced P–P coupling in uranium chemistry is less common,[10] although P–P coupling processes have been generally observed in the field of main-group elements or transition metals,[11] or even in rare-earth metals.[12] Herein, we report a reversible P–P bond formation in a uranium-based redox-active multidentate nitrogen–phosphorous (N–P) ligand.

The multidentate N–P ligand **1** was readily synthesized by the reaction of bis(2-aminophenyl)amine with two equivalents of ^{i}Pr$_2$PCl in the presence of DBU (see the ESI†). The ^{31}P{^{1}H} NMR spectrum of compound **1** in C_6D_6 exhibits a resonance peak at 46.24 ppm, which is consistent with the signal for the multidentate N–P ligands previously reported by our group.[13] Treatment of two molecules of **1** with six equivalents of KHMDS at −30 °C in THF for 2 h (Scheme 1), followed by the addition of one equivalent of UCl_4 and then stirring at RT for another 4 h, gave a dark brown solution. An *in situ* ^{1}H NMR spectrum reveals that a single uranium product was formed in this reaction (Fig. S4, ESI†), but complex **2** was isolated only in 29% crystallized yield after workup. The ^{31}P{^{1}H} NMR spectrum of complex **2** shows a singlet peak at −474.56 ppm. The ^{1}H NMR spectrum of complex **2** has six resonances in the range from +56.35 to −12.88 ppm, which suggests a highly symmetrical structure in solution.

The solid-state molecular structure of complex **2** was elucidated by single-crystal X-ray diffraction (Fig. 1). The uranium center is supported by two multidentate N–P ligands, and there is a weak interaction between two potassium ions and phenyl groups on ligands. The U–N bond lengths are in the range of 2.321(5)–2.426(5) Å, which are consistent with the U–N_{amido} bond lengths reported previously.[14,15] The U–P distances are in the range of 3.158(2)–3.450(2) Å, which are longer than the sum of the single bond covalent radii for U and P (2.81 Å),[16] but are very close to the U–P distances reported in uranium complexes supported by the similar N–P scaffold ligands.[14,17]

Under the same conditions, when ^{n}BuLi was used as the deprotonation reagent in the reaction of compound **1** with UCl_4

[a] *State Key Laboratory of Coordination Chemistry, Jiangsu Key Laboratory of Advanced Organic Materials, School of Chemistry and Chemical Engineering, Nanjing University, Nanjing 210093, China. E-mail: zcq@nju.edu.cn*

[b] *LPCNO, CNRS & INSA, Université Paul Sabatier, 135 Avenue de Rangueil, 31077 Toulouse, France. E-mail: laurent.maron@irsamc.ups-tlse.fr*

† Electronic supplementary information (ESI) available. CCDC 2102548 and 2102549. For ESI and crystallographic data in CIF or other electronic format see DOI: 10.1039/d1cc04765e

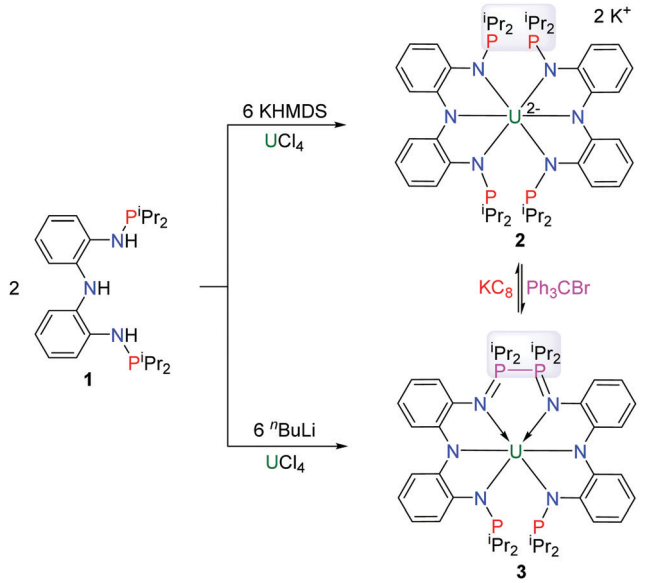

Scheme 1 Synthesis of complexes **2** and **3**.

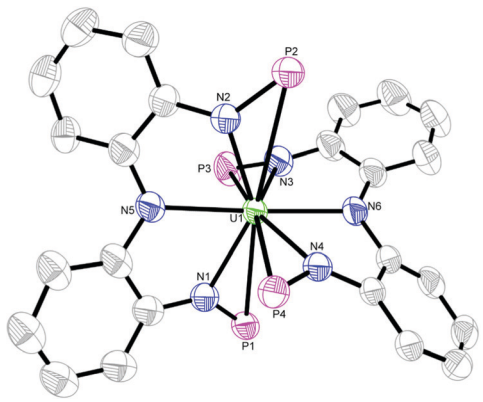

Fig. 1 Molecular structure for the cation of complex **2** with 50% probability ellipsoids. Hydrogen atoms and isopropyl moieties in P^iPr_2 are omitted for clarity.

(Scheme 1), the *in situ* ^{1}H NMR spectrum exhibits signals that differ markedly from those of complex **2** (Fig. S5, ESI†). Complex **3** was isolated in 29% yield as a brown crystalline solid from this reaction. The ^{1}H NMR spectrum of pure complex **3** reveals 20 paramagnetically shifted resonances ranging from +66.18 to −59.41 ppm. The $^{31}P\{^1H\}$ NMR spectrum displays two singlet peaks at +811.42 and −635.59 ppm, suggesting the P atoms in two distinct chemical environments. Note that there is no P–P coupling reaction when reacting compound **1** with ^{n}BuLi in the absence of UCl_4 (Fig. S6, ESI†). These results indicate that the different deprotonation reagents result in different products in these reactions.

X-Ray quality crystals of complex **3** were grown in a saturated toluene solution at −35 °C and the structural features of complex **3** were elucidated by X-ray crystallography (Fig. 2). The most salient feature of complex **3** is a new P–P bond. The length of this P2–P3 bond is 2.272(3) Å, which is very close to the sum of the

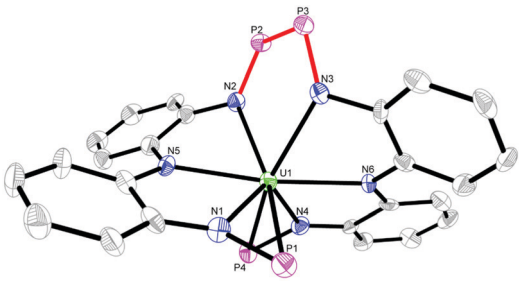

Fig. 2 Molecular structure for complex **3** with 50% probability ellipsoids. Hydrogen atoms and isopropyl moieties in P^iPr_2 are omitted for clarity.

single bond covalent radii of two P atoms (2.22 Å).[16] The bond lengths of U1–N2 (2.497(7) Å) and U1–N3 (2.494(7) Å) are obviously longer than the other U–N bond lengths, which range from 2.308(7) to 2.398(7) Å, suggesting that U1–N2 and U1–N3 are coordinate bonds. Meanwhile, the bond distances of P3–N3 (1.593(8) Å) and P2–N2 (1.606(7) Å) are obviously shorter than the other P–N bonds whose lengths are in the range of 1.650(7)–1.666(7) Å. The lengths of the P3–N3 and P2–N2 bonds are shorter than the sum of the double-bond covalent radii for P and N atoms (1.62 Å),[16] and consequently they exhibit some double bond character and the formal oxidation states for P2 and P3 atoms have been increased from +III to +V. The disproportionation of UCl_4 precursor seems possible in this process, which was consistent with the low isolated yield for complex **3**.[18]

The most important structural difference between complexes **2** and **3** is the formation of a P–P bond *via* the oxidation of P atoms. Thus, when treating complex **2** with an oxidant, Ph_3CBr, in THF at RT for 3 h, complex **3** was formed cleanly as shown in the *in situ* ^{1}H NMR spectrum (Fig. S11, ESI†). A mechanism with the phosphide radical[11a,11c] was proposed for the formation of complex **3** from **2**. Interestingly, complex **3** can be converted to **2** *via* P–P bond cleavage under reductive conditions (Scheme 1). Upon treatment of complex **3** with excess KC_8 in THF at RT for 4 h, the golden color of KC_8 faded and complex **2** was formed, as confirmed by the *in situ* ^{1}H NMR spectrum (Fig. S12, ESI†). However, no conversion of **2** to **3** or of **3** to **2** was obtained after heating or exposure to light. Therefore, a redox-induced reversible P–P coupling was achieved in a uranium system by employing a novel multidentate N–P ligand.

To investigate the oxidation state of the U center in complexes **2** and **3**, variable-temperature magnetic data were measured with a super-conducting quantum interference device (SQUID) in the solid state. The RT magnetic moments of complexes **2** and **3** are 3.75 and 3.77 μ_B, respectively, which are close to the expected value (3.58 μ_B) for U(IV) ions at RT. With decreasing temperature, the magnetic moments of **2** and **3** steadily decrease to 0.70 and 0.78 μ_B at 1.8 K, respectively, and tend toward zero in each case (Fig. 3). The magnitude and temperature dependence of magnetic moments for complexes **2** and **3** are consistent with a $5f^2$ U(IV) center with a $^3H_4$ configuration.[15] This result clearly indicates that the N–P units on the ligand are involved in the redox process during the

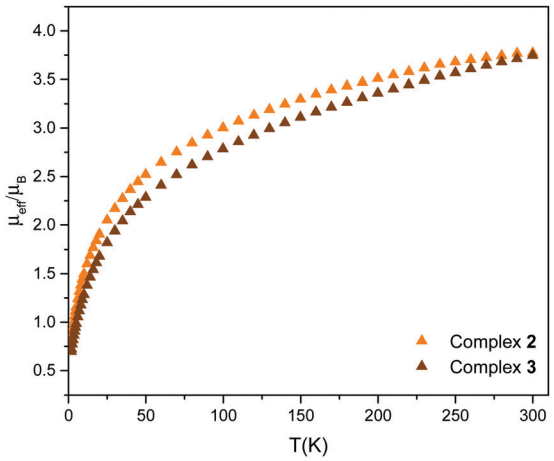

Fig. 3 Variable-temperature magnetic moment data for **2** and **3**.

conversion between **2** and **3**, rather than a redox phenomenon on the uranium center.

Complexes **2** and **3** exhibit similar UV-visible-NIR electronic absorption spectra in THF solution. They have intense absorption peaks at 303 and 304 nm, respectively, which can be assigned to charge-transfer bands. In the NIR region, both **2** and **3** display several dominant, but weak absorption peaks ($\varepsilon < 60$ M^{-1} cm^{-1}), attributed to f–f transitions which are expected for U(IV) species. The absorption spectra of **2** and **3** are consistent with the U(IV) formulations and further confirmed that the redox process occurred on the N–P units rather than on the uranium center (Fig. 4).

To gain further insight into the transformation of complex **2** to complex **3**, density functional theory (DFT) calculations were performed using the B3PW91 functional. The oxidation of the anionic part of complex **2** onto $\mathbf{2^{ox}}$ is computed to be favored by 17.8 kcal mol^{-1} in the presence of Ph_3CBr. Then the transformation of $\mathbf{2^{ox}}$ onto **3** is found to be a reversible process (Fig. 5). An intermediate **Int1**, which only the orientation of one

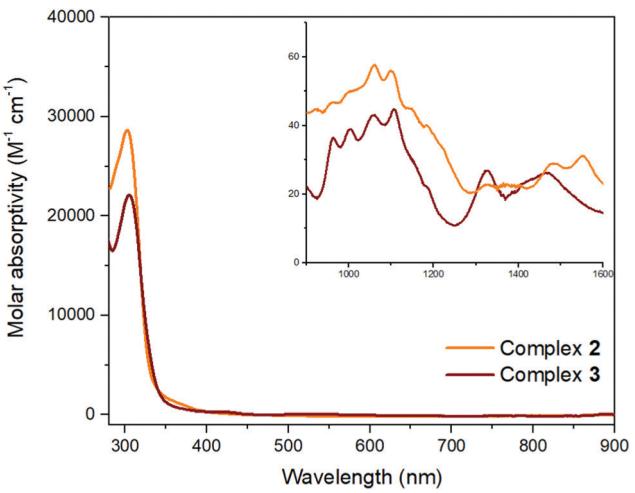

Fig. 4 UV-visible-NIR absorption spectra of complexes **2** and **3** measured in THF at RT. Inset: NIR absorption spectra.

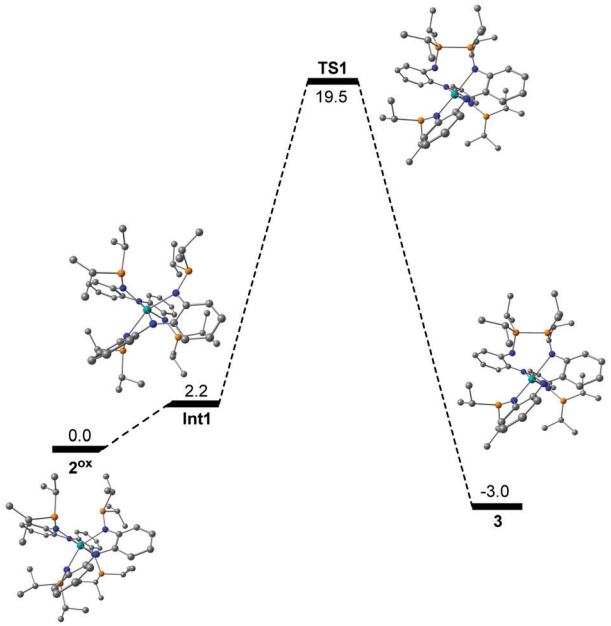

Fig. 5 Energy profile (kcal mol^{-1}) for the reversible P–P coupling between $\mathbf{2^{ox}}$ and **3**.

phosphine was different with $\mathbf{2^{ox}}$, was located (2.2 kcal mol^{-1}). An accessible P–P coupling transition state (TS, 19.5 kcal mol^{-1}) was located on the potential energy surface and is consistent with a kinetically facile reaction. At **TS1**, the long (3.00 Å) P–P bond connects one phosphorus with a trigonal planar arrangement with the second phosphorus that has a trigonal pyramidal geometry. Therefore, the σ lone pair on the bent phosphorus in **2** undergoes a nucleophilic attack on the empty p orbital of the flat phosphorus, and this explains the moderate height of the barrier. Following the intrinsic reaction coordinate it yields complex **3** in which the fully formed P–P bond is 2.30 Å in length, in good agreement with the experimentally observed 2.27 Å, while the P–N bond length was found to be 1.62 Å. The natural bonding orbital analysis on the bonding indicates the formation of a covalent P–P single bond as well as the presence of two polarized P=N double bonds. The formation of complex **3** is only slightly exothermic (3.0 kcal mol^{-1}).

In summary, two uranium(IV) complexes **2** and **3** were isolated by the reactions of the multidentate N–P ligand **1** with UCl_4 with different deprotonation reagents, KHMDS and ^{n}BuLi. Reversible P–P bond formation and cleavage of these complexes were observed in the presence of an oxidant (Ph_3CBr) or a reductant (KC_8). DFT calculations indicate that this occurs by a nucleophilic attack of one phosphorus to the other one. This study not only highlights the different behaviors of KHMDS and ^{n}BuLi in uranium chemistry but also provides a novel redox-active N–P scaffold.

This research was supported by the National Natural Science Foundation of China (Grant No. 21772088 and 91961116) and Programs for high-level entrepreneurial and innovative talents introduction of Jiangsu Province (individual and group programs). L. M. is a senior member of the Institut Universitaire de France. Humboldt Foundation and Chinese Academy of Science

are acknowledged for financial support. CalMip is also gratefully acknowledged for a generous grant of computing time.

Conflicts of interest

The authors declare no competing financial interests.

Notes and references

1 (*a*) O. R. Luca and R. H. Crabtree, *Chem. Soc. Rev.*, 2013, **42**, 1440–1459; (*b*) B. Ding, M. B. Solomon, C. F. Leong and D. M. D'Alessandro, *Coord. Chem. Rev.*, 2021, **439**, 213891; (*c*) X. Wang, Z. Mo, J. Xiao and L. Deng, *Inorg. Chem.*, 2013, **52**, 59–65; (*d*) P. Cui and V. M. Iluc, *Chem. Sci.*, 2015, **6**, 7343–7354; (*e*) D. Zhu, I. Thapa, I. Korobkov, S. Gambarotta and P. H. M. Budzelaar, *Inorg. Chem.*, 2011, **50**, 9879–9887; (*f*) D. Wang, X. Leng, S. Ye and L. Deng, *J. Am. Chem. Soc.*, 2019, **141**, 7731–7735; (*g*) C. A. Gould, E. Mu, V. Vieru, L. E. Darago, K. Chakarawet, M. I. Gonzalez, S. Demir and J. R. Long, *J. Am. Chem. Soc.*, 2020, **50**, 21197–21209.

2 (*a*) D. P. Halter, F. W. Heinemann, L. Maron and K. Meyer, *Nat. Chem.*, 2018, **10**, 259–267; (*b*) S. J. Kraft, U. J. Williams, S. R. Daly, E. J. Schelter, S. A. Kozimor, K. S. Boland, J. M. Kikkawa, W. P. Forrest, C. N. Christensen, D. E. Schwarz, P. E. Fanwick, D. L. Clark, S. D. Conradson and S. C. Bart, *Inorg. Chem.*, 2011, **50**, 9838–9848; (*c*) S. J. Kraft, P. E. Fanwick and S. C. Bart, *Inorg. Chem.*, 2010, **49**, 1103–1110; (*d*) J. J. Kiernicki, B. S. Newell, E. M. Matson, N. H. Anderson, P. E. Fanwick, M. P. Shores and S. C. Bart, *Inorg. Chem.*, 2014, **53**, 3730–3741; (*e*) J. H. Farnaby, T. Chowdhury, S. J. Horsewill, B. Wilson and F. Jaroschik, *Coord. Chem. Rev.*, 2021, **437**, 213830; (*f*) G. B. Panetti, J. R. Robinson, E. J. Schelter and P. J. Walsh, *Acc. Chem. Res.*, 2021, **54**, 2637–2648.

3 (*a*) N. H. Anderson, S. O. Odoh, Y. Yao, U. J. Williams, B. A. Schaefer, J. J. Kiernicki, A. J. Lewis, M. D. Goshert, P. E. Fanwick, E. J. Schelter, J. R. Walensky, L. Gagliardi and S. C. Bart, *Nat. Chem.*, 2014, **6**, 919–926; (*b*) E. J. Coughlin, Y. Qiao, E. Lapsheva, M. Zeller, E. J. Schelter and S. C. Bart, *J. Am. Chem. Soc.*, 2019, **141**, 1016–1026; (*c*) S. A. Pattenaude, C. S. Kuehner, W. L. Dorfner, E. J. Schelter, P. E. Fanwick and S. C. Bart, *Inorg. Chem.*, 2015, **54**, 6520–6527.

4 J. R. Pankhurst, N. L. Bell, M. Zegke, L. N. Platts, C. A. Lamfsus, L. Maron, L. S. Natrajan, S. Sproules, P. L. Arnold and J. B. Love, *Chem. Sci.*, 2017, **8**, 108–116.

5 (*a*) M. J. Monreal and P. L. Diaconescu, *J. Am. Chem. Soc.*, 2010, **132**, 7676–7683; (*b*) M. J. Monreal, S. Khan and P. L. Diaconescu, *Angew. Chem., Int. Ed.*, 2009, **48**, 8352–8355.

6 C. Camp, V. Mougel, P. Horeglad, J. Pécaut and M. Mazzanti, *J. Am. Chem. Soc.*, 2010, **132**, 17374–17377.

7 B. Kosog, C. E. Kefalidis, F. W. Heinemann, L. Maron and K. Meyer, *J. Am. Chem. Soc.*, 2012, **134**, 12792–12797.

8 L. Zhang, G. Hou, G. Zi, W. Ding and M. D. Walter, *J. Am. Chem. Soc.*, 2016, **138**, 5130–5142.

9 G. T. Kent, J. Murillo, G. Wu, S. Fortier and T. W. Hayton, *Inorg. Chem.*, 2020, **59**, 8629–8634.

10 J. Du, D. Hunger, J. A. Seed, J. D. Cryer, D. M. King, A. J. Wooles, J. Slageren and S. T. Liddle, *J. Am. Chem. Soc.*, 2021, **143**, 5343–5348.

11 (*a*) Y.-E. Kim and Y. Lee, *Angew. Chem., Int. Ed.*, 2018, **57**, 14159–14163; (*b*) P. M. Scheetz, D. S. Glueck and A. L. Rheingold, *Organometallics*, 2017, **36**, 3387–3397; (*c*) L. N. Grant, B. Pinter, B. C. Manor, R. Suter, H. Gretzmacher and D. J. Mindiola, *Chem. – Eur. J.*, 2017, **23**, 6272–6276; (*d*) J. J. Weigand, N. Burford and A. Decken, *Eur. J. Inorg. Chem.*, 2008, 4343–4347; (*e*) H. Schneider, D. Schmidt and U. Radius, *Chem. Commun.*, 2015, **51**, 10138–10141; (*f*) L. J. Taylor, M. Bühl, B. A. Chalmers, M. J. Ray, P. Wawrzyniak, J. C. Walton, D. B. Cordes, A. M. Z. Slawin, J. Derek Woollins and P. Kilian, *J. Am. Chem. Soc.*, 2017, **139**, 18545–18551; (*g*) Z. Wang, N. Asok, J. Gaffen, Y. Gottlieb, W. Bi, C. Gendy, R. Dobrovetsky and T. Baumgartner, *Chem*, 2018, **4**, 2628–2643; (*h*) C. Taube, K. Schwedtmann, M. Noikham, E. Somsook, F. Hennersdorf, R. Wolf and J. J. Weigand, *Angew. Chem., Int. Ed.*, 2020, **59**, 3585–3591.

12 Y. Lv, C. E. Kefalidis, J. Zhou, L. Maron, X. Leng and Y. Chen, *J. Am. Chem. Soc.*, 2013, **135**, 14784–14796.

13 (*a*) G. Feng, M. Zhang, D. Shao, X. Wang, S. Wang, L. Maron and C. Zhu, *Nat. Chem.*, 2019, **11**, 248–253; (*b*) X. Xin, I. Douair, Y. Zhao, S. Wang, L. Maron and C. Zhu, *J. Am. Chem. Soc.*, 2020, **142**, 15004–15011; (*c*) G. Feng, K. N. McCabe, S. Wang, L. Maron and C. Zhu, *Chem. Sci.*, 2020, **11**, 7585–7592; (*d*) X. Xin and C. Zhu, *Dalton Trans.*, 2020, **49**, 603–607; (*e*) P. Wang, I. Douair, Y. Zhao, S. Wang, J. Zhu, L. Maron and C. Zhu, *Angew. Chem., Int. Ed.*, 2021, **60**, 473–479.

14 B. M. Gardner and S. T. Liddle, *Chem. Commun.*, 2015, **51**, 10589–10607.

15 D. R. Kindra and W. J. Evans, *Chem. Rev.*, 2014, **114**, 8865–8882.

16 (*a*) P. Pyykkö and M. Atsumi, *Chem. – Eur. J.*, 2009, **15**, 186–197; (*b*) P. Pyykkö, *J. Phys. Chem. A*, 2015, **119**, 2326–2337.

17 (*a*) J. W. Napoline, S. J. Kraft, E. M. Matson, P. E. Fanwick, S. C. Bart and C. M. Thomas, *Inorg. Chem.*, 2013, **52**, 12170–12177; (*b*) A. L. Ward, W. W. Lukens, C. C. Lu and J. Arnold, *J. Am. Chem. Soc.*, 2014, **136**, 3647–3654.

18 (*a*) A. L. Odom, P. L. Arnold and C. C. Cummins, *J. Am. Chem. Soc.*, 1998, **120**, 5836–5837; (*b*) P. L. Arnold, A. J. Blake and C. Wilson, *Chem. – Eur. J.*, 2005, **11**, 6095–6099; (*c*) S. Duhović, S. Khan and P. L. Diaconescu, *Chem. Commun.*, 2010, **46**, 3390–3392; (*d*) O. J. Cooper, J. McMaster, W. Lewis, A. J. Blake and S. T. Liddle, *Dalton Trans.*, 2010, **39**, 5074–5076; (*e*) J. T. Boronski, L. R. Doyle, J. A. Seed, A. J. Wooles and S. T. Liddle, *Angew. Chem., Int. Ed.*, 2020, **59**, 295–299.

